

Bioinformatics analysis reveals the key factors affecting the progress of osteoporosis

Hao Huang^{1, 2}, Wenhao Tang^{1, 2}, Chengliang Yang^{2, *}

¹ Youjiang Medical College for Nationalities, Baise Guangxi, China

² Affiliated Hospital of Youjiang Medical College for Nationalities, Baise, Guangxi, China

*Corresponding Author: stbyyl@126.com

ABSTRACT

The incidence rate of osteoporosis is high, and patients usually have decreased bone density and increased risk of fracture, which seriously affects their quality of life. This study aims to reveal key biomarkers that affect the progression of osteoporosis through bioinformatics methods. This study selected the GSE91033 and GSE93883 datasets for analysis, and obtained differentially expressed miRNAs using the GEO2R analysis tool; Predicting potential miRNA target factors through miRDIP and conducting pathway enrichment analysis of target factors through DAVID database; Analyze the interaction relationships between target factors through the STRING database, and construct a protein interaction network and a miRNA mRNA interaction network. The results showed that 73 and 79 differentially expressed genes were obtained in the GSE91033 and GSE93883 datasets, respectively. Common genes included hsa-miR-4508, hsa-miR-660-5p, and hsa-miR-424-5p. Pathway enrichment analysis showed that downstream target factors of differentially expressed miRNAs involved PIK/AKT, Wnt, Hippo, MAPK, and NF-κB pathway is closely related to cell proliferation and differentiation, and also involves intracellular phosphorylation activity. Protein interaction analysis revealed that CCND1, WEE1, MAP2K1, BTRC, FGF2, AXIN2, PTCH1, CCND2, KIF5C, DYNC111 and PAFAH1B1 are node genes involved in the progression of osteoporosis. The miRNA mRNA interaction network revealed that hsa-miR-424-5p is a key factor affecting the progression of osteoporosis.

KEYWORDS

Osteoporosis; Bioinformatics; Markers; MiRNA

1. INTRODUCTION

Osteoporosis is a common chronic orthopedic disease, which is mostly found in the elderly or postmenopausal women [1, 2]. Most patients are characterized by a decrease in bone density and abnormal microscopic bone structure, which leads to an increase in bone fragility, which leads to an increase in the risk of fracture [3, 4]. The dynamic stability of osteoblasts and osteoclasts is an important condition for maintaining the soundness of normal human bones. The destruction of homeostasis between osteoblasts and osteoblasts is the main cause of the progression of many orthopedic diseases [5, 6]. Studies have confirmed that the reduction of osteoblast production or abnormal proliferation of osteoclasts will lead to the gradual loss of bone, which will lead to the formation of osteoporosis in patients [7, 8] A large number of studies have confirmed that abnormal cell proliferation and apoptosis activity caused by the disorder of the expression of some key genes in bone cells is the main cause of the progression of osteoporosis [9, 10]. However, so far, the mechanism of the progress of osteoporosis has not been fully clarified.

MicroRNA is a class of small RNA with a length of 20-24 nucleotides, which is widely found in eukaryotic cells and participates in a variety of life activities such as mammalian cell proliferation, differentiation, metabolism and apoptosis [11, 12]. The disorder of miRNA expression is closely related to the formation and development of many diseases [13]. Some differentially expressed miRNAs are often used as serum markers for the screening and diagnosis of patients' early diseases [14]. Studies have confirmed that compared with normal people, there are significant differences in the expression of miRNA in skeletal cells of patients with osteoporosis. Some miRNA can affect the expression of some key genes by targeting mRNA, resulting in abnormal metabolic activity in bone cells, causing the destruction of the dynamic balance of osteoblasts/osteoplasts, thus promoting bone loss in patients [15].

This study intends to reveal the changes of miRNA expression in the progression of elderly patients with osteoporosis through bioinformatics analysis, screen the key factors affecting the progression of osteoporosis, and provide a reference basis for the early diagnosis and clinical treatment of osteoporosis.

2. METHODS

2.1. Data Collection

The data sets used in this study are all derived from the GEO open source database, and the GSE91033 and GSE93883 data sets are used to analyze bioinformatics analysis.

2.2. Analysis of Differential Genes

Analyze the GSE91033 and GSE93883 data sets through the GEO2R tool provided by the GEO database to obtain the difference expression matrix. The genes of $\text{adj.P.value} < 0.05$ and $|\text{LogFC}| \geq 2$ are screened as differential expression genes for further analysis. The same genes are screened through the intersection of differential expression genes in the GSE91033 and GSE93883 data sets through the Wein diagram. The downstream target protein of miRNA is predicted through the mirDIP online database (<http://ophid.utoronto.ca/mirDIP/index.jsp>) and the protein with very high score class is screened as a potential target factor.

2.3. Functional Enrichment

Annotate and enrich differential expression genes and miRNA prediction target genes through the DAVID online database, and obtain GO analysis and KEGG analysis records. Filter the enrichment function or path of $\text{adj.P.value} < 0.05$.

2.4. Network Analysis Of Mirna-Mrna And Protein Interaction

Protein interaction analysis was carried out on the potential targets of differential expression of mRNA and miRNA prediction in GSE91033 and GSE93883 data set. The interaction between proteins is revealed through the STRING online database (<https://cn.string-db.org/>). The structure diagram of miRNA-mRNA and protein interaction network is constructed through Cytoscape software.

3. RESULTS

3.1. Screening of Differential Gene Expression

According to the screening criteria, 73 and 79 differential expression genes were obtained from the GSE91033 and GSE93883 data sets respectively. Among them, the GSE91033 data set contains 22 up-adjusted genes and 57 down-adjusted genes, the GSE93883 data set contains 21 up-adjusted genes and 52 down-adjusted genes (**Figure 1 A-B**). The results of Wayne graph analysis show that the GSE91033 and GSE93883 data sets contain three common differential expression genes, including hsa-miR-4508, hsa-miR-660-5p and hsa-miR-424-5p (**Figure 1 C**).

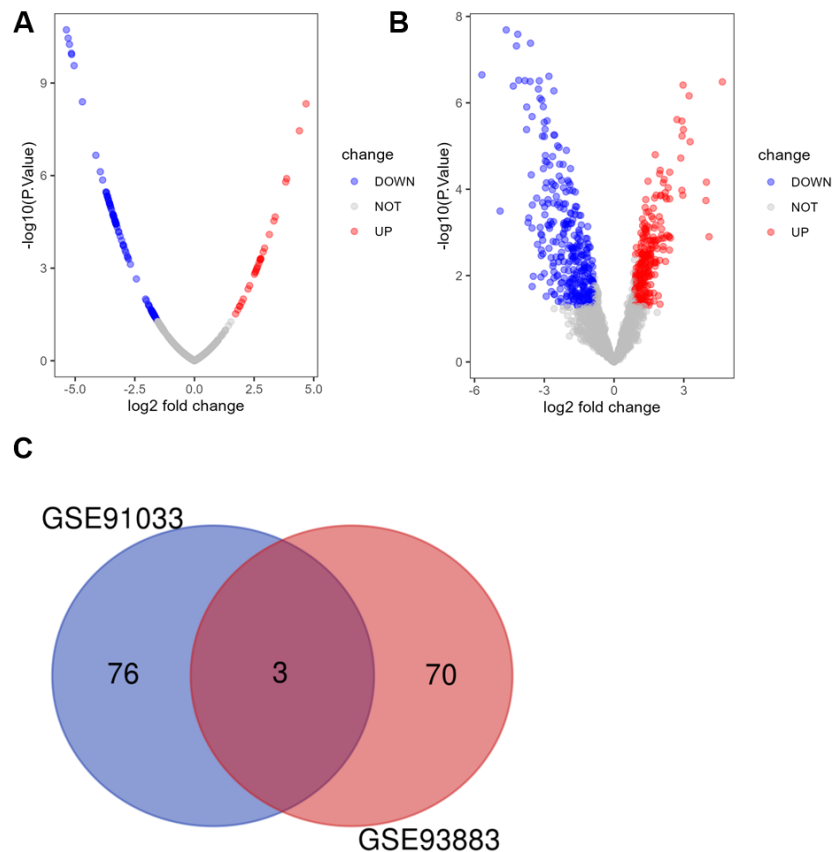


Figure 1. The differentially expressed miRNA in GSE91033 and GSE93883

(A) The differentially expressed miRNA in GSE91033; (B) The differentially expressed miRNA in GSE93883; (C) The common gene of GSE91033 and GSE93883

3.2. The Enrichment of Functions and Signal Channels

The study predicted the target protein of differential expression of miRNA through the mirDIP database, obtained 116 common proteins, and carried out functional and pathway enrichment of downstream predicted target proteins through the DAVID database, and screened the pathway of $p < 0.05$. As shown in **Figure 2**, the proteins that differentially express miRNA downstream involve the regulation of multiple signaling pathways in cells, including PIK/AKT, Wnt, Hippo, MAPK and NF- κ B. The results of GO enrichment analysis show that the downstream target of differential expression of miRNA involves cell life activities such as cell proliferation regulation, development, intracellular phosphorylation pathway and cell differentiation. In addition, these protein factors have serine/threonine/tyrosine kinase activity and may participate in post-translational modifications such as intracellular phosphorylation (Table 1).

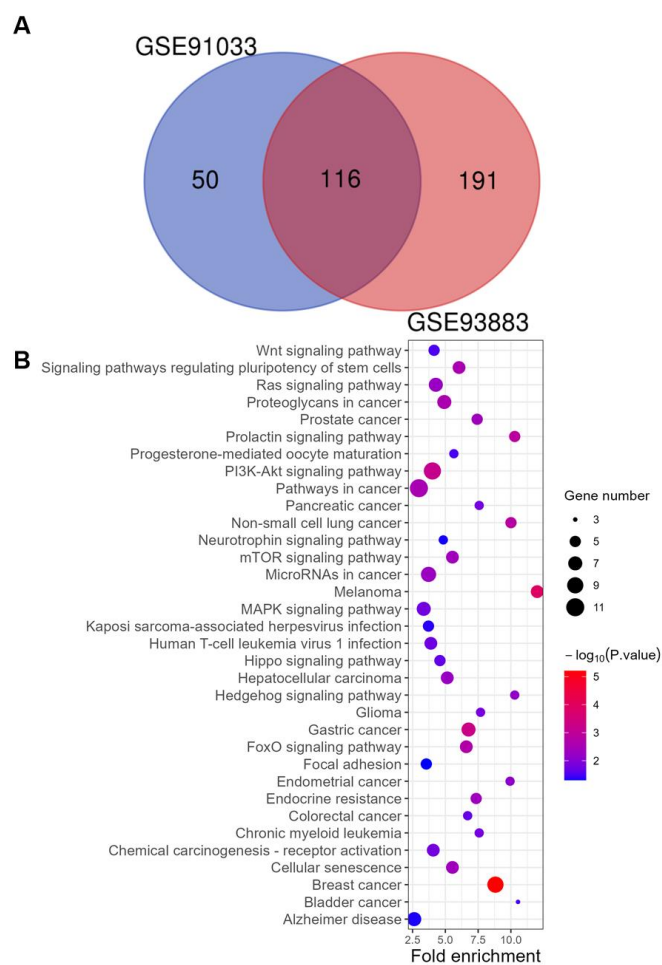


Figure 2. The KEGG enrichment of targets predicted by miRDIP

(A) The common targets of miRNA in GSE91033 and GSE93883; (B) KEGG enrichment of common targets

Table 1. GO enrichment of the common targets of miRNA in GSE91033 and GSE93883

Term	Discription	PValue	Genes
GO:0006468	protein phosphorylation	4.06E-04	CDK17, MAP2K1, WEE1, CCNT2, INSR, AKT3, TLK1, SGK1, ACVR2A, FGFR1
GO:0030509	BMP signaling pathway	0.001357821	TMEM100, USP15, PDCD4, ACVR2A, SMAD7
GO:0006511	ubiquitin-dependent protein catabolic process	0.003430646	USP25, USP15, RNF217, UBE4B, RBBP6, BTRC, FBXO21
GO:0016567	protein ubiquitination	0.003712883	UBE2Q1, RNF138, FBXW7, RNF217, UBE4B, RBBP6, BTRC, SOCS6, WDTC1
GO:0048812	neuron projection morphogenesis	0.004319878	WEE1, SLC9A6, BDNF, SGK1
GO:0048665	neuron fate specification	0.004956365	EYA1, MYT1L, DLL1
GO:0001934	positive regulation of protein phosphorylation	0.005734878	CCND2, CCND1, INSR, AXIN2, FGF2, ACVR2A
GO:0008284	positive regulation of cell proliferation	0.006260027	PURA, GAREM1, CNOT6L, CCND2, INSR, E2F3, DLL1, FGF2, FGFR1
GO:1905564	positive regulation of vascular endothelial cell proliferation	0.008719668	AKT3, FGF2, FGFR1
GO:0043433	negative regulation of sequence-specific DNA binding transcription factor activity	0.011265885	PURA, PTCH1, BTRC, SMAD7
GO:0097421	liver regeneration	0.014158798	CCND1, PTCH1, PTPN3
GO:0060070	canonical Wnt signaling pathway	0.014859306	EDA, RECK, FGF2, LRP6
GO:0090049	regulation of cell migration	0.015038109	FBXW7, FGF2
GO:0016055	involved in sprouting angiogenesis	0.017032645	CCND1, RNF138, AXIN2, BTRC, LRP6
GO:0048513	Wnt signaling pathway	0.017303442	EDA, FGF2, FGFR1
GO:0006974	animal organ development	0.017444841	BTG2, CCND1, FBXW7, TLK1, RBBP6, SGK1
	cellular response to DNA damage stimulus		

GO:0007405	neuroblast proliferation	0.01813181	BTG2, FGF2, PAFAH1B1
GO:2000546	positive regulation of endothelial cell chemotaxis to fibroblast growth factor protein	0.020000899	FGF2, FGFR1
GO:0000209	polyubiquitination	0.020065117	UBE2Q1, FBXW7, RNF217, UBE4B, BTRC
GO:0001658	branching involved in ureteric bud morphogenesis	0.020715241	EYA1, PTCH1, FGF2
GO:0045944	positive regulation of transcription from RNA polymerase II promoter	0.02085517	CCNT2, PID1, EYA1, PLAG1, ASH1L, DLL1, FGF2, ACVR2A, LRP6, RPS6KA3, DMTF1, MYB, E2F3
GO:0072089	stem cell proliferation	0.022517647	PTCH1, AXIN2, FGF2
GO:0006325	chromatin organization	0.023467965	USP25, EYA1, TLK1, ASH1L, RSBN1, PHF19
GO:0001701	in utero embryonic development	0.024118929	TMEM100, YTHDC1, PTCH1, RBBP6, WDTC1
GO:0031547	brain-derived neurotrophic factor receptor signaling pathway	0.024938938	SLC9A6, BDNF
GO:0043536	positive regulation of blood vessel endothelial cell migration	0.025337856	AKT3, FGF2, FGFR1
GO:0043161	proteasome-mediated ubiquitin-dependent protein catabolic process	0.026697105	FBXW7, UBE4B, AXIN2, BTRC, CD2AP
GO:0060011	Sertoli cell proliferation	0.029852347	BCL2L2, ACVR2A
GO:0000079	regulation of cyclin-dependent protein serine/threonine kinase activity	0.030337504	CCNT2, CCND2, CCND1
GO:0045893	positive regulation of	0.030550954	RAP2C, USP25, MAP2K1, INSR, PTCH1, MYB, BTRC, FGF2, LRP6

GO:0000122	transcription, DNA-templated negative regulation of transcription from RNA polymerase II promoter fibroblast growth factor receptor signaling pathway	0.031902477	PURA, BTG2, TGIF2, CCND1, MYT1L, DNAJB4, PTCH1, MYB, PHF19, SMAD7, WDTC1
GO:0008543	cell cycle	0.03459436	SHOC2, FGF2, FGFR1
GO:0007049	response to ischemia	0.037696779	RPS6KA3, CCNT2, DMTF1, TLK1, CD2AP, PAFAH1B1
GO:0002931	cell division	0.043749315	MYB, CPEB2, BCL2L2
GO:0051301	MAPK cascade	0.044357152	WEE1, CCNT2, CCND2, CCND1, CD2AP, PAFAH1B1
GO:0000165	positive regulation of gene expression	0.044999188	MAP2K1, ASH1L, FGFR1, PTPN3
GO:0010628	G1/S transition of mitotic cell cycle	0.047280255	MAP2K1, EDA, PID1, PLAG1, MED26, DLL1, FGF2
GO:0000082	mammary gland epithelial cell proliferation	0.047389882	CCND2, CCND1, E2F3
GO:0033598	positive regulation of phospholipase C activity	0.049262115	CCND1, BTRC
GO:0010863	negative regulation of neuron apoptotic process	0.049262115	FGF2, FGFR1
GO:0043524		0.049334331	BTG2, CCND1, BDNF, CPEB2
GO:0005829	cytosol	3.85E-07	BTG2, AHCYL2, CCNT2, GPR63, ARHGAP5, FBXO21, RPS6KA3, PCMT1, CCND2, UBE2Q1, CCND1, MYB, BTRC, MAP2K1, CNOT6L, FBXW7, KIF23, WIP1, AXIN2, CD2AP, RAP2C, DMTF1, CSDE1, SGK1, PAFAH1B1, USP15, STXB3, PLAG1, CDCA4, PPM1D, DNAJB4, RNF217, MAP7, CDC37L1, RBBP6, SHOC2, SOCS6, N4BP1, DYNC1I1, WDTC1, USP25, PRRC2C, HELZ, SMAD7, CLCN5, SYNJ1, CAPZA2, PDCD4,

GO:0005634	nucleus	1.33E-05	<p>BCL2L2, PTPN3, TNRC6B, FGFR1</p> <p>BTG2, CCNT2, MYT1L, FGF2, GPATCH8, CCND2, UBE2Q1, CCND1, AKT3, MYB, TLK1, BTRC, MAP2K1, TGIF2, CNOT6L, FBXW7, KIF23, UBE4B, ASH1L, AXIN2, MED26, RSBN1, DMTF1, SGK1, PAFAH1B1, USP15, LUZP1, PLAG1, YTHDC1, CDCA4, ARL3, PPM1D, PURA, RNF138, RBBP6, E2F3, SHOC2, N4BP1, DYNC1I1, CDK17, USP25, EYA1, PTCH1, XPO7, HELZ, SMAD7, WEE1, PDCD4, CPEB2, PHF19, FGFR1 MOB4, TMEM100, CCNT2, SYNJ1, BDNF, FBXW7, PTCH1, MAP7, CPEB2, DYNC1I1, CD2AP, PAFAH1B1</p>
GO:0048471	perinuclear region of cytoplasm	0.001057534	<p>BTG2, USP15, PID1, LUZP1, ARL3, ARHGAP5, FGF2, RPS6KA3, PCMT1, CCND2, CCND1, KIF5C, AKT3, RNF217, CDC37L1, SHOC2, SOCS6, BTRC, DYNC1I1, WDTC1, CDK17, USP25, CNOT6L, SPRYD3, EYA1, BDNF, FBXW7, XPO7, KIF23, UBE4B, AXIN2, ACVR2A, CD2AP, SMAD7, RAP2C, MOB4, WEE1, PDCD4, TBPL1, SGK1, CPEB2, PTPN3, PAFAH1B1</p>
GO:0005737	cytoplasm	0.0017236	<p>USP15, CCNT2, PLAG1, YTHDC1, CDCA4, ARL3, GPR63, PPM1D, RPS6KA3, CCND2, CCND1, DNAJB4, MYB, TLK1, E2F3, SHOC2, BTRC, WDTC1, USP25, TGIF2, EYA1, FBXW7, KIF23, WIPI2, ASH1L, MED26, SMAD7, WEE1, DMTF1, NUP50, SGK1, TNRC6B, PHF19</p>
GO:0005654	nucleoplasm	0.002474529	

GO:0005813	centrosome	0.006892249	TGIF2, LUZP1, PLAG1, ARL3, KIF23, RBBP6, AXIN2, PAFAH1B1, SMAD7
GO:0005874	microtubule	0.022475945	SYNJ1, KIF5C, MAP7, KIF23, DYNC1I1, PAFAH1B1
GO:0005871	kinesin complex	0.025385989	KIF5C, KIF23, PAFAH1B1
GO:0043025	neuronal cell body	0.038212904	MOB4, PURA, KIF5C, KCNJ2, PAFAH1B1, LRP6
GO:0005770	late endosome	0.040209665	MAP2K1, SLC9A6, RASGEF1B, INSR, BTG2, AHCYL2, CCNT2, EDA, PID1, ARHGAP5, FGF2, GPATCH8, TMEM100, RPS6KA3, PCMT1, CCND2, UBE2Q1, CCND1, KIF5C, AKT3, MYB, TLK1, BTRC, MAP2K1, CNOT6L, FBXW7, KIF23, WIPI2, AXIN2, FAM91A1, MED26, CD2AP, RAP2C, GAREM1, SLC9A6, CSDE1, NUP50, PAPPA, PLSCR4, TBPL1, SGK1, PAFAH1B1, USP15, STXBP3, YTHDC1, CDCA4, ARL3, PPM1D, DLL1, LRP6, PURA, RNF138, DNAJB4, MAP7, CDC37L1, RBBP6, E2F3, SHOC2, SOCS6, KCNJ2, N4BP1, DYNC1I1, WDTC1, CDK17, USP25, EYA1, BDNF, INSR, PTCH1, PRRC2C, XPO7, C1ORF21, HELZ, ACVR2A, SMAD7, MOB4, CLCN5, WEE1, SYNJ1, CAPZA2, PDCD4, RECK, BCL2L2, PTPN3, PHF19, TNRC6B, FGFR1
GO:0005515	protein binding	2.60E-04	
GO:0004712	protein serine/threonine/tyrosine kinase activity	0.002261868	CDK17, RPS6KA3, MAP2K1, WEE1, INSR, AKT3, TLK1, SGK1, FGFR1
GO:0061575	cyclin-dependent protein kinase activator activity	0.003085698	CCNT2, CCND2, CCND1
GO:0004674	protein serine/threonine kinase activity	0.004975549	CDK17, RPS6KA3, MAP2K1, AKT3, TLK1, PPM1D, SGK1, ACVR2A

GO:0016538	cyclin-dependent protein serine/threonine kinase regulator activity	0.012081481	CCNT2, CCND2, CCND1
GO:0008013	beta-catenin binding	0.01238857	AXIN2, BTRC, CD2AP, SMAD7
GO:0044877	macromolecular complex binding	0.012993769	CCND1, SYNJ1, STXBP3, INSR, PTCH1, BCL2L2, CD2AP
GO:0004672	protein kinase activity	0.014996617	CDK17, RPS6KA3, MAP2K1, WEE1, CCND1, AKT3, TLK1
GO:1904928	coreceptor activity involved in canonical Wnt signaling pathway	0.015578003	RECK, LRP6
GO:0090722	receptor-receptor interaction	0.020717097	FGF2, FGFR1
GO:0004713	protein tyrosine kinase activity	0.0218586	MAP2K1, WEE1, INSR, FGFR1
GO:0005524	ATP binding	0.028693853	CDK17, MAP2K1, INSR, HELZ, KIF23, ACVR2A, RPS6KA3, CLCN5, WEE1, UBE2Q1, KIF5C, AKT3, TLK1, SGK1, FGFR1
GO:0015026	coreceptor activity	0.030198022	RECK, ACVR2A, LRP6
GO:1990756	protein binding, bridging involved in substrate recognition for ubiquitination	0.034605394	FBXW7, BTRC, SMAD7
GO:0003777	microtubule motor activity	0.039245885	KIF5C, KIF23, DYNC1I1

3.3. Analysis of Protein Interaction Network

The study carried out mutual analysis of 116 potential target proteins of predicted miRNA through STRING online database, and screened 11 node proteins, including *CCND1*, *WEE1*, *MAP2K1*, *BTRC*, *FGF2*, *AXIN2*, *PTCH1*, *CCND2*, *KIF5C*, *DYNC1I1* and *PAFAH1B1*, and revealed the interaction relationship through cytoscape (Figure 3-4).

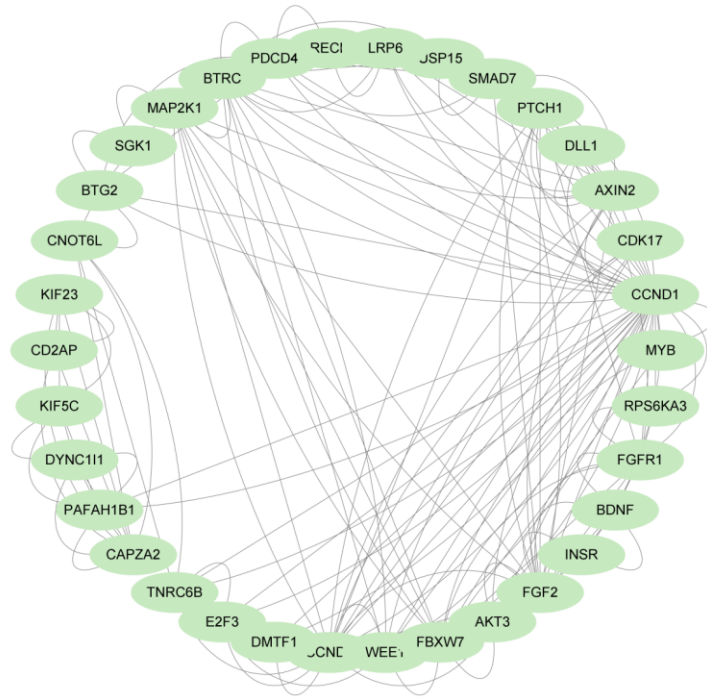


Figure 3. Protein-interaction-network of targets analyzed by STRING database

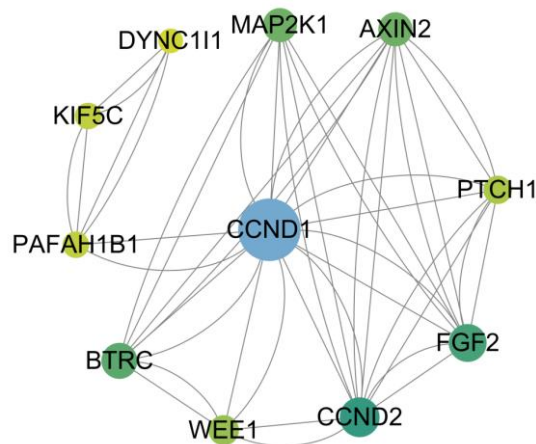


Figure 4. Protein-interaction-network of key node genes

3.4. Analysis of miRNA-mRNA interaction network

The study constructed hsa-miR-424-5p and its downstream target genes or relationships through Cytoscape (as shown in **Figure 5**). hsa-miR-424-5p has a potential interaction with 102 proteins such as *CCND1*, *WEE1*, *MAP2K1*, *BTRC*, *FGF2*, *AXIN2*, *PTCH1*, *CCND2*, *KIF5C*, *DYNC111* and *PAFAH1B1*.

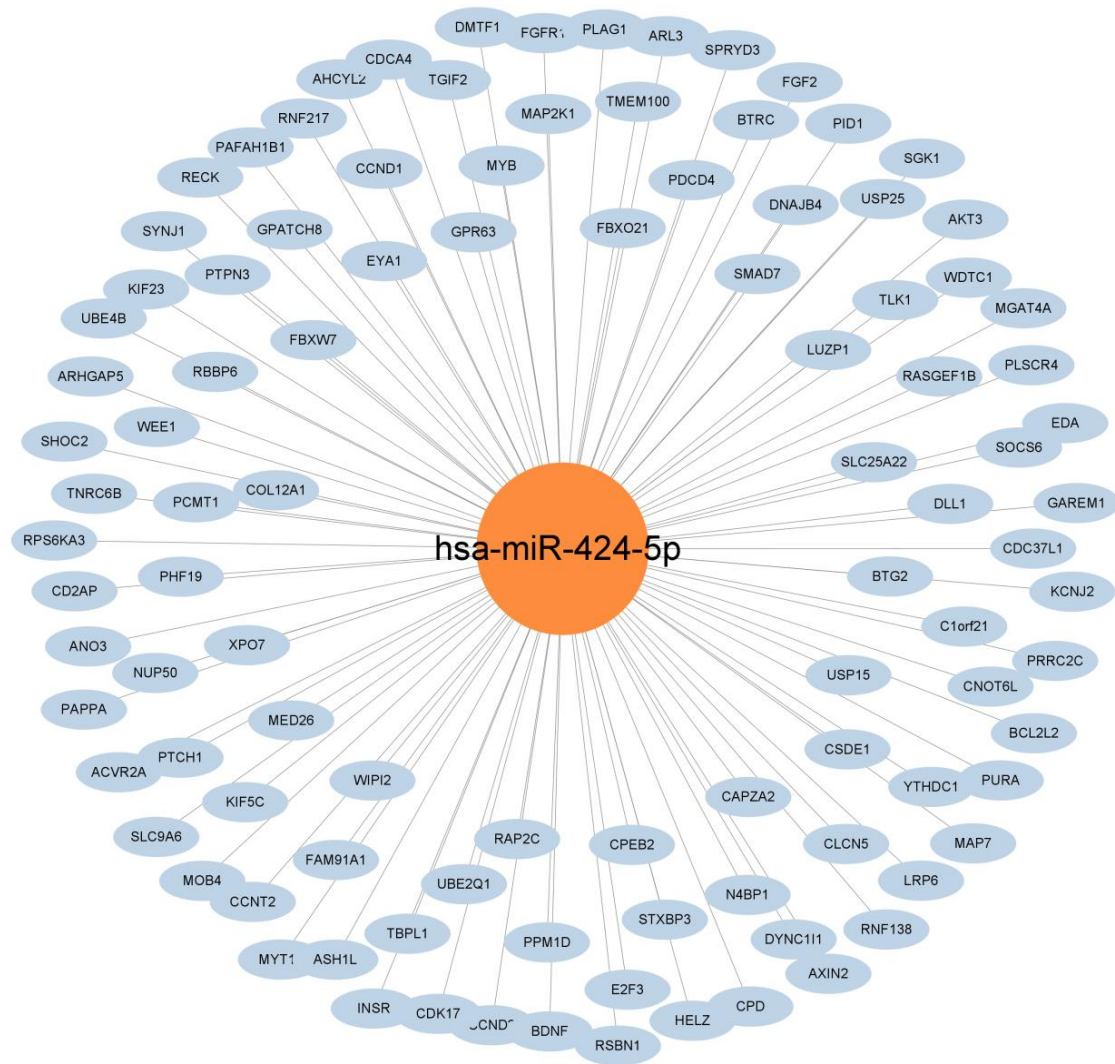


Figure 5. miRNA-mRNA network

4. DISCUSSION

The formation and development of osteoporosis are closely related to the life activities of osteoblasts and osteoblasts proliferation, differentiation and apoptosis of patients. By analyzing GSE91033 and GSE93883 data sets, this study found significant abnormal expression of hsa-miR-4508, hsa-miR-660-5p and hsa-miR-424-5p in the lesion tissue of patients with osteoporosis. miR-660-5p and miR-424-5p were confirmed to be related to the progression of osteoporosis. The miR-660-5p uphanging has been confirmed to be potentially associated with cell proliferation. miR-660-5p can promote the proliferation of non-small cell lung cancer and other cells by activating the PI3K/AKT pathway [16]. In the GSE91033 and GSE93883 data sets, the expression of miR-660-5p is significantly downged. Elena et al. found that miR-660-5p was significantly reduced in serum samples of patients with osteoporosis. These results show that miR-660-5p may maintain the proliferation of osteoblasts by activating the PI3K/AKT pathway, and its downward regulation will lead to the block of bone formation, which will lead to osteoporosis [17]. miR-424-5p plays an important regulatory role in many diseases [18, 19]. miR-424-5p can inhibit the inflammatory response of endometrial epithelial cells induced by lipopolysaccharides by targeting *IRAK2* [20]. *In addition*, a number of studies have confirmed that miR-424-5p plays an important role in maintaining cell proliferation capacity by regulating multiple signaling pathways. This study found that miR-424-5p in patient samples was significantly lowered. miR-424-5p has been shown to affect osteoblast differentiation by regulating the Wnt signaling pathway [21].

By analyzing the enrichment of differential expression gene pathways, this study found that differential genes involve multiple signaling pathways. Osteoporosis is closely related to the imbalance of multiple signaling pathways in bone cells. PI3K/AKT signaling pathway is an intracellular signal transduction pathway, which also responds to extracellular signals and promotes cell proliferation, metabolism and growth. Its abnormalities are closely related to a variety of orthopedic diseases [22, 23]. Studies have confirmed that the disorder of PI3K/AKT signaling pathway is an important cause of the progress of osteoporosis. Some studies have pointed out that the activation of the PI3K/AKT signaling pathway can relieve steroid-induced osteoporosis by inhibiting bone mesenchymal stem cell wire [24]. In this study, path enrichment analysis found that the abnormal expression of *MAP2K1*, *CCND2*, *CCND1*, *BDNF*, *INSR*, *AKT3*, *MYB*, *SGK1*, *FGF2* and *FGFR1* is closely related to PI3K/AKT pathway imbalance. The Wnt signaling pathway participates in a variety of biological activities such as embryonic development, cell proliferation and cell differentiation [25]. The abnormality of Wnt signaling pathway is closely related to the formation and progression of cancer and other diseases [26]. The disorder of Wnt signaling pathway is also directly related to the progression of osteoporosis. The Wnt signaling pathway is involved in the proliferation, differentiation and apoptosis of chondrocytes, mesenchymal hepatocytes, osteoblasts and osteoclasts, thus affecting the bone development process [27]. Wnt signaling pathway disorder can lead to proliferation and apoptosis of osteoblasts and osteoblasts. Studies have pointed out that Dkk-1 and SOST can block the Wnt signaling pathway, inhibit the proliferation and differentiation of osteoblasts, and disrupt the dynamic balance between osteoblasts and osteoblasts, thus promoting the progress of osteoporosis [28]. In addition, the activation of the Wnt signaling pathway can inhibit the development of osteoclasts, inhibit bone absorption, and increase bone density [29]. In this study, it was found through gene enrichment that proteins such as *CCND2*, *CCND1*, *AXIN2*, *BTRC* and *LRP6* were related to the Wnt signaling pathway. The Hippo pathway is a highly conservative intracellular signal transduction mechanism, which is essential for the regulation of a variety of vital activities such as cell proliferation, differentiation and metabolism [30]. This study found that the abnormal expression of *CCND2*, *CCND1*, *AXIN2*, *BTRC* and *SMAD7* is related to the Hippo pathway. In addition, pathway enrichment results show that genes such as *MAP2K1*, *BDNF*, *INSR*, *AKT3*, *FGF2* and *FGFR1* are related to the MAPK oxidative stress signaling pathway. The pathway of abnormal oxidative stress-mediated apoptosis of osteoclasts has been proved to be a key factor in the progression of osteoporosis. Increased levels of oxidative stress in osteoclasts will activate the NF- κ B signaling pathway through the MAPK pathway to activate the apoptosis signaling pathway in osteoblasts and mediate cell apoptosis, thus maintaining the homeostasis between osteoblasts/osteocytes in the bone [31].

This study screened some key node proteins through the protein interaction network, including *CCND1*, *WEE1*, *MAP2K1*, *BTRC*, *FGF2*, *AXIN2*, *PTCH1*, *CCND2*, *KIF5C*, *DYNC111* and *PAFAH1B1*. *CCND1* plays an important role in the proliferation of osteoblasts [32]. Some studies have pointed out that *CCND1* has an inhibitory effect on the progression of osteoporosis, while miR-23b-3p can promote the progression of osteoporosis by targeting *CCND1* [33]. *AXIN2* is one of the key factors in the Wnt signal pathway [34]. Duan et al. found that miR-16-5p can promote the progression of osteoporosis by inhibiting *AXIN2* expression [35]. *FGF2* has been proven to play an important role in the progression of osteoporosis. Wen et al. found that *FGF2* can promote the development of osteoporosis by activating the ERK-CREB signaling pathway [36]. In addition, the miRNA-mRNA interaction network reveals that hsa-miR-424-5p has a potential interaction relationship with 102 proteins, which is a potential marker affecting the progress of osteoporosis.

In summary, this study supports miR-424-5p as a key factor affecting the progress of osteoporosis, and its downstream factors *CCND1*, *WEE1*, *MAP2K1*, *BTRC*, *FGF2*, *AXIN2*, *PTCH1*, *CCND2*, *KIF5C*, *DYNC111* and *PAFAH1B1* are the key node factors affecting the onset of the disease.

Funding

There's no funding here.

Ethics Approval and Consent to Participate

Not applicable.

Consent for Publication

Not applicable.

Competing Interests

The authors declare that they have no competing interests.

Data Availability Statement

Data openly available in a public repository.

Author Contributions

Conceptualization: Hao HUANG, Wenhao Tang and Chengliang Yang;

Formal analysis: Hao HUANG, Wenhao Tang and Chengliang Yang;

Methodology: Hao HUANG, Wenhao Tang and Chengliang Yang;

Project administration: Hao HUANG, Wenhao Tang and Chengliang Yang;

Software: Hao HUANG, Wenhao Tang and Chengliang Yang;

Writing-original draft: Hao HUANG, Wenhao Tang and Chengliang Yang.

REFERENCES

- [1] BEHERA J, ISON J, VOOR M J, et al. Exercise-Linked Skeletal Irisin Ameliorates Diabetes-Associated Osteoporosis by Inhibiting the Oxidative Damage-Dependent miR-150-FNDC5/Pyroptosis Axis [J]. *Diabetes*, 2022, 71(12): 2777-92.
- [2] QASEEM A, FORCIEA M A, MCLEAN R M, et al. Treatment of Low Bone Density or Osteoporosis to Prevent Fractures in Men and Women: A Clinical Practice Guideline Update From the American College of Physicians [J]. *Ann Intern Med*, 2017, 166(11): 818-39.
- [3] REN L J, ZHU X H, TAN J T, et al. MiR-210 improves postmenopausal osteoporosis in ovariectomized rats through activating VEGF/Notch signaling pathway [J]. *BMC Musculoskelet Disord*, 2023, 24(1): 393.
- [4] MA T L, ZHU P, KE Z R, et al. Focusing on OB-OC-MΦ Axis and miR-23a to Explore the Pathogenesis and Treatment Strategy of Osteoporosis [J]. *Front Endocrinol (Lausanne)*, 2022, 13: 891313.
- [5] YU T, YOU X, ZHOU H, et al. MiR-16-5p regulates postmenopausal osteoporosis by directly targeting VEGFA [J]. *Aging (Albany NY)*, 2020, 12(10): 9500-14.
- [6] LEE K S, LEE J, KIM H K, et al. Extracellular vesicles from adipose tissue-derived stem cells alleviate osteoporosis through osteoprotegerin and miR-21-5p [J]. *J Extracell Vesicles*, 2021, 10(12): e12152.
- [7] FU Y, XU Y, CHEN S, et al. MiR-151a-3p Promotes Postmenopausal Osteoporosis by Targeting SOCS5 and Activating JAK2/STAT3 Signaling [J]. *Rejuvenation Res*, 2020, 23(4): 313-23.
- [8] WANG J, GAO Z, GAO P. MiR-133b Modulates the Osteoblast Differentiation to Prevent Osteoporosis Via Targeting GNB4 [J]. *Biochem Genet*, 2021, 59(5): 1146-57.
- [9] WANG W W, YANG L, WU J, et al. The function of miR-218 and miR-618 in postmenopausal osteoporosis [J]. *Eur Rev Med Pharmacol Sci*, 2017, 21(24): 5534-41.
- [10] WANG W W, YANG L, WU J, et al. The function of miR-218 and miR-618 in postmenopausal osteoporosis [J]. *Eur Rev Med Pharmacol Sci*, 2017, 21(24): 5534-41.
- [11] LIU H P, HAO D J, WANG X D, et al. MiR-30a-3p promotes ovariectomy-induced osteoporosis in rats via targeting SFRP1 [J]. *Eur Rev Med Pharmacol Sci*, 2019, 23(22): 9754-60.
- [12] AN H, CHU C, ZHANG Z, et al. Hyperoside alleviates postmenopausal osteoporosis via regulating miR-19a-5p/IL-17A axis [J]. *Am J Reprod Immunol*, 2023, 90(1): e13709.
- [13] MA J, LIN X, CHEN C, et al. Circulating miR-181c-5p and miR-497-5p Are Potential Biomarkers for Prognosis and Diagnosis of Osteoporosis [J]. *J Clin Endocrinol Metab*, 2020, 105(5).

- [14] DING M, LIU B, CHEN X, et al. MiR-99b-5p suppressed proliferation of human osteoblasts by targeting FGFR3 in osteoporosis [J]. *Hum Cell*, 2021, 34(5): 1398-409.
- [15] YOU Y, LIU J, ZHANG L, et al. WTAP-mediated m(6)A modification modulates bone marrow mesenchymal stem cells differentiation potential and osteoporosis [J]. *Cell Death Dis*, 2023, 14(1): 33.
- [16] ZHANG X, ZHU Y, ZHANG C, et al. miR-542-3p prevents ovariectomy-induced osteoporosis in rats via targeting SFRP1 [J]. *J Cell Physiol*, 2018, 233(9): 6798-806.
- [17] LI L, ZHENG B, ZHANG F, et al. LINC00370 modulates miR-222-3p-RGS4 axis to protect against osteoporosis progression [J]. *Arch Gerontol Geriatr*, 2021, 97: 104505.
- [18] WANG Z, ZHANG H, LI Q, et al. Long non-coding RNA KCNQ1OT1 alleviates postmenopausal osteoporosis by modulating miR-421-3p/mTOR axis [J]. *Sci Rep*, 2023, 13(1): 2333.
- [19] ZHAO W, DONG Y, WU C, et al. MiR-21 overexpression improves osteoporosis by targeting RECK [J]. *Mol Cell Biochem*, 2015, 405(1-2): 125-33.
- [20] UMAR T, MA X, YIN B, et al. miR-424-5p overexpression inhibits LPS-stimulated inflammatory response in bovine endometrial epithelial cells by targeting IRAK2 [J]. *J Reprod Immunol*, 2022, 150: 103471.
- [21] WEI Y, MA H, ZHOU H, et al. miR-424-5p shuttled by bone marrow stem cells-derived exosomes attenuates osteogenesis via regulating WIF1-mediated Wnt/ β -catenin axis [J]. *Aging (Albany NY)*, 2021, 13(13): 17190-201.
- [22] LI M, YANG N, HAO L, et al. Melatonin Inhibits the Ferroptosis Pathway in Rat Bone Marrow Mesenchymal Stem Cells by Activating the PI3K/AKT/mTOR Signaling Axis to Attenuate Steroid-Induced Osteoporosis [J]. *Oxid Med Cell Longev*, 2022, 2022: 8223737.
- [23] LI S, CUI Y, LI M, et al. Acteoside Derived from Cistanche Improves Glucocorticoid-Induced Osteoporosis by Activating PI3K/AKT/mTOR Pathway [J]. *J Invest Surg*, 2023, 36(1): 2154578.
- [24] LI M, YANG N, HAO L, et al. Melatonin Inhibits the Ferroptosis Pathway in Rat Bone Marrow Mesenchymal Stem Cells by Activating the PI3K/AKT/mTOR Signaling Axis to Attenuate Steroid-Induced Osteoporosis [J]. *Oxid Med Cell Longev*, 2022, 2022: 8223737.
- [25] CANALIS E. Wnt signalling in osteoporosis: mechanisms and novel therapeutic approaches [J]. *Nat Rev Endocrinol*, 2013, 9(10): 575-83.
- [26] RACHNER T D, KHOSLA S, HOFBAUER L C. Osteoporosis: now and the future [J]. *Lancet*, 2011, 377(9773): 1276-87.
- [27] RONG X, KOU Y, ZHANG Y, et al. ED-71 Prevents Glucocorticoid-Induced Osteoporosis by Regulating Osteoblast Differentiation via Notch and Wnt/ β -Catenin Pathways [J]. *Drug Des Devel Ther*, 2022, 16: 3929-46.
- [28] GAO Y, CHEN N, FU Z, et al. Progress of Wnt Signaling Pathway in Osteoporosis [J]. *Biomolecules*, 2023, 13(3).
- [29] MAEDA K, KOBAYASHI Y, KOIDE M, et al. The Regulation of Bone Metabolism and Disorders by Wnt Signaling [J]. *Int J Mol Sci*, 2019, 20(22).
- [30] YANG W, HAN W, QIN A, et al. The emerging role of Hippo signaling pathway in regulating osteoclast formation [J]. *J Cell Physiol*, 2018, 233(6): 4606-17.
- [31] XIAO L, ZHONG M, HUANG Y, et al. Puerarin alleviates osteoporosis in the ovariectomy-induced mice by suppressing osteoclastogenesis via inhibition of TRAF6/ROS-dependent MAPK/NF- κ B signaling pathways [J]. *Aging (Albany NY)*, 2020, 12(21): 21706-29.
- [32] WANG L J, CAI H Q. Let-7b downgrades CCND1 to repress osteogenic proliferation and differentiation of MC3T3-E1 cells: An implication in osteoporosis [J]. *Kaohsiung J Med Sci*, 2020, 36(10): 775-85.
- [33] WANG J Z, ZHAO B H. MiR-23b-3p functions as a positive factor for osteoporosis progression by targeting CCND1 in MC3T3-E1 cells [J]. *In Vitro Cell Dev Biol Anim*, 2021, 57(3): 324-31.
- [34] LIN Z, ZHENG J, CHEN J, et al. Antiosteoporosis Effect and Possible Mechanisms of the Ingredients of Fructus Psoraleae in Animal Models of Osteoporosis: A Preclinical Systematic Review and Meta-Analysis [J]. *Oxid Med Cell Longev*, 2021, 2021: 2098820.
- [35] DUAN J, LI H, WANG C, et al. BMSC-derived extracellular vesicles promoted osteogenesis via Axin2 inhibition by delivering MiR-16-5p [J]. *Int Immunopharmacol*, 2023, 120: 110319.
- [36] WEN X, HU G, XIAO X, et al. FGF2 positively regulates osteoclastogenesis via activating the ERK-CREB pathway [J]. *Arch Biochem Biophys*, 2022, 727: 109348.